

# 1 APPLICATION OF LIBS TECHNOLOGY FOR DETERMINATION OF CL 2 CONCENTRATIONS IN MORTAR SAMPLES

3 J. Mateo<sup>1</sup>, M.C. Quintero<sup>1</sup>, J.M. Fernández<sup>2</sup>, M.C. García<sup>1</sup>, A. Rodero<sup>1\*</sup>

4 <sup>1</sup>Grupo de Física de Plasmas: Diagnósis, Modelos y Aplicaciones (FQM-136). Edificio  
5 Einstein (C-2), Campus de Rabanales. Universidad de Córdoba, 14071 Córdoba, Spain

6 <sup>2</sup>Departamento de Química Inorgánica e Ingeniería Química. Escuela Politécnica Superior  
7 de Belmez. Avenida de la Universidad s/n. 14240 Belmez, Córdoba, Spain.

8 \*Author for correspondence, e-mail: fa1rosea@uco.es

## 9 10 **Abstract**

11 In a society where the cement and concrete industry is of great importance, the diagnosis  
12 of the quality of these materials has become a matter of highest priority. One of the  
13 maximum exponents of the deterioration of a reinforced concrete structure is the chloride  
14 ion content. In this work it has been shown that its evaluation, traditionally carried out by  
15 chemical methods, can also be performed by laser-induced breakdown spectroscopy  
16 (LIBS), a much faster and advantageous technique. This work develops an optimal  
17 experimental set-up based on the generation of small discharges using a 532 nm Nd:YAG  
18 laser of 320 mJ, in a helium atmosphere. The experimental conditions have been optimized  
19 and a calibration curve, relating the ratio of intensities of Cl I 837.60 nm and Ca II 849.80  
20 nm obtained from the LIBS and the actual chloride concentration, has been determined  
21 from a set of samples with different ion chloride concentrations. These samples have been  
22 simultaneously subjected to a traditional chemical analysis, as well as instrumental  
23 contrast analysis using energy-dispersive X-ray spectroscopy (EDX). Finally, LIBS  
24 technique has been applied to the study of mortar samples that had been submerged in

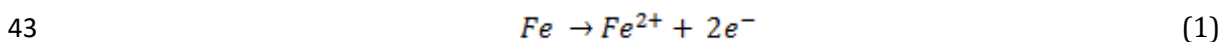
25 saturated sea salt water for 60 months, and in this way their average ion chloride  
26 concentration and their depth profiles have been obtained.

27 **Keywords:** Laser-induced breakdown spectroscopy, atomic emission, chloride content,  
28 mortar corrosion, building materials

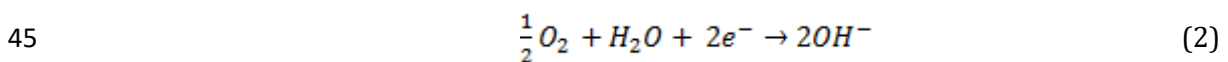
## 29 **1. Introduction**

30 Mortar and concrete are the most important materials used in building and  
31 construction. Concrete industry involves millions of dollars, being one of the basis of the  
32 modern society development. It is well known that environmental conditions can affect  
33 these materials. The presence of aggressive elements in air and water produces continued  
34 degradation of the structures what eventually results in their spalling and final collapse.  
35 One of the most harmful elements is the chloride ion which particularly affects reinforced  
36 concrete structures. Chloride ions cause localized depassivation of the reinforcing steel  
37 and its later corrosion. These ions may be introduced in the concrete either during the  
38 manufacturing process or by its exposure to external agents including pollution, marine  
39 environments or de-icing salts.

40 The corrosion of reinforcing steel in concrete structures is an electrochemical process  
41 [1-2], due to the electron current between an anodic and a cathodic area in the bars, given  
42 by the following half-cell reactions:

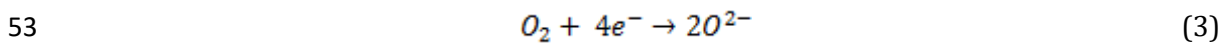


44 which is the anodic oxidation of Fe from the steel bars, and



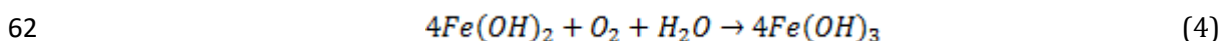
46 which is the cathodic reduction with H<sub>2</sub>O present in the inner hole and O<sub>2</sub> from the air  
47 diffusion through the concrete.

48 In the absence of chloride ions the pH of the concrete is about 12-13, due to the  
49 presence of calcium, potassium and sodium hydroxides. Under these alkaline conditions, a  
50 stable film of the Fe oxides Fe<sub>2</sub>O<sub>3</sub> and Fe<sub>3</sub>O<sub>4</sub> is formed thus passivating the surface of the  
51 bars of reinforcing steel:



56 Corrosion reactions (1) and (2) are avoided as long as this passivation film exists.

57 In the presence of chloride ion, the passivation film is locally destroyed and then  
58 processes of localized corrosion are again initiated. If there is not enough oxygen,  
59 reactions (3) are not produced, giving instead ferric hydroxide through the following  
60 reactions:



64 The accumulation of these corrosion products taking a volume several times larger  
65 than that of the original iron (almost 600% higher) results in the cracking and spalling of  
66 the concrete cover.

67 The corrosion process has been studied by several authors. A parameter of special  
68 interest is the so-called *chloride threshold level*, defined as the chloride concentration at  
69 the steel/concrete interface resulting in a significant corrosion. Glass and other authors  
70 report experimental values obtained under different conditions [3-4]. From those values it  
71 was shown that the total chloride content, expressed in wt. % cement, is in the range of  
72 0.17-2.5.

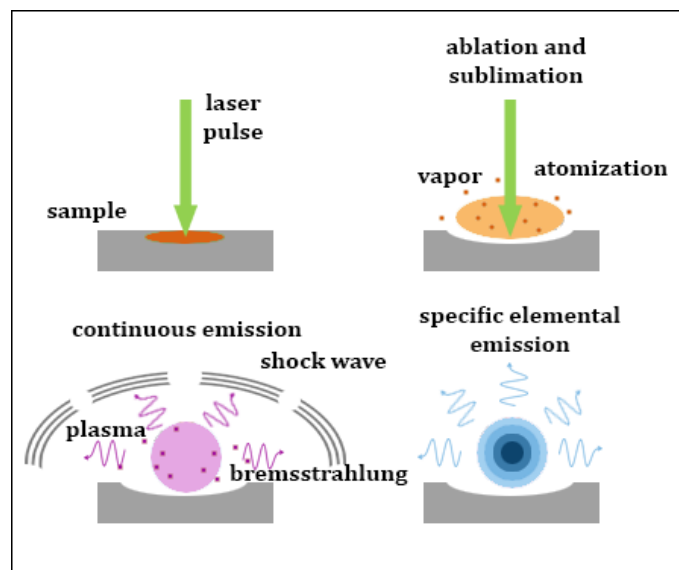
73 Thus, to know the chloride concentration and whether or not its values are over  
74 threshold levels is important to know about the corrosion state of reinforced concrete, in  
75 order to avoid the collapse of structures with an early prediction.

76 Among all the existing techniques to determine Cl concentration of mortar and  
77 concrete, those based on chemical analysis are much extended. The Volhard's method is  
78 one of the most used for this kind of materials. It consists on an indirect argentometry, i.e.  
79 an indirect titration to determine the chloride ion that precipitates with silver ion. It was  
80 described for the first time by Jacob Volhard in 1874. However, despite giving reliable  
81 quantitative results, chemical analysis has the drawback of being a destructive method, as  
82 it requires to reduce the sample to dust in order to carry out the determination. Besides,  
83 these methods are time-consuming as samples need to be transported to the laboratory,  
84 and previous adaptation of the samples is also needed.

85 In this work LIBS technique has been used for the determination of Cl concentration  
86 in mortar and concrete, as an alternative method to chemical analysis. LIBS technique is  
87 based on the spectral analysis of the optical emission of the plasma generated by the  
88 interaction of a laser pulse with the surface of the sample [5-6]. This interaction is mainly  
89 ruled by the electronic properties of the solid, so that the light can be reflected,  
90 transmitted or absorbed. During absorption, under the action of the laser, the free  
91 electrons oscillate and interact with the crystalline lattice, producing a transfer of heat,  
92 followed by a diffusion of that heat in the solid phase. The resulting effect is a balance

93 between the heat gain, produced by the laser, and the losses given by thermal diffusion. In  
94 this balance the duration of the pulse is a key parameter.

95 When a high energy laser is used, the surface of the sample is melted and vaporized  
96 (Fig. 1), resulting in the phenomenon of ablation. A number of atoms and electrons are  
97 removed from the surface, producing an acceleration of these electrons by the inverse  
98 bremsstrahlung effect as a result of their interaction with the laser. The atoms are ionized  
99 by the collision with these accelerated electrons, so that the number of electrons increases  
100 exponentially, producing the ignition of a plasma. The plasma produced in LIBS is a  
101 transient plasma, so that the excitation of the particles decreases with time after the laser  
102 pulse. As it is a highly ionized plasma, its emission spectrum shows a strong background  
103 radiation and highly broadened lines (due to Stark effect) during the first microseconds  
104 after the laser pulse. Because of this, in LIBS measurements, delay generators must be  
105 used for the signal to be detected in a certain period of time after laser pulse, in order to  
106 avoid this Stark effect, and to ensure that the laser energy has completely dissipated and  
107 cannot damage the measuring instruments. Thus, LIBS measurements are taken in the  
108 vapor of excited atoms formed right after the plasma phase.



109  
110

Fig. 1 –Fundamentals of LIBS technique.

111 This process is followed by a relaxation phase, where the excited atoms return to  
112 their ground state, emitting energy in the form of photons that are characteristic of each  
113 element. This energy is associated with a line at a given position in the spectrum, whose  
114 intensity depends directly on the energy of the photon and the number of photons  
115 emitted. Also, the number of photons emitted is directly proportional to the number of  
116 atoms excited in that energy level and to the probability of that electronic transition. The  
117 number of atoms excited at that energy level and the total number of atoms of the  
118 considered element are directly related by the Boltzmann equation.

119 Unlike other spectroscopic techniques, LIBS technique has the advantage of being able  
120 to analyze any substance regardless of its state of aggregation, whether solids, liquids,  
121 gases, or even colloids such as aerosols, gels and other types of samples. Because all  
122 elements of the periodic table emit light when they are properly excited, LIBS technique  
123 can potentially solve the elemental composition of any sample, its capacity being mainly  
124 limited by the power of the laser, the spectral resolution of the spectrometer and the  
125 detector sensitivity.

126 LIBS systems, in their different modalities (simple pulse, multiple pulse, double laser,  
127 etc.), have been integrated in the research laboratories as a response to the demand for  
128 systems capable of performing fast, non-destructive elemental analysis, and that provide  
129 accurate quantitative information on the analyte. Thus, thanks to the simplicity of the LIBS  
130 set-up, it can be found in many fields, with industrial, environmental, biomedicine,  
131 archeology, metallurgy or forensic science applications [7-13]. Data obtained from LIBS can  
132 be analyzed by using several methods, including artificial neural networks as an  
133 alternative to the traditional calibration methods [14-15].

134 Some authors have previously reported on the use of LIBS for the analysis of building  
135 material using single and double lasers [16-24]. Wilsch et al. showed the linear relationship  
136 between intensity of atomic lines of Cl and its concentration in mortar, showing that this

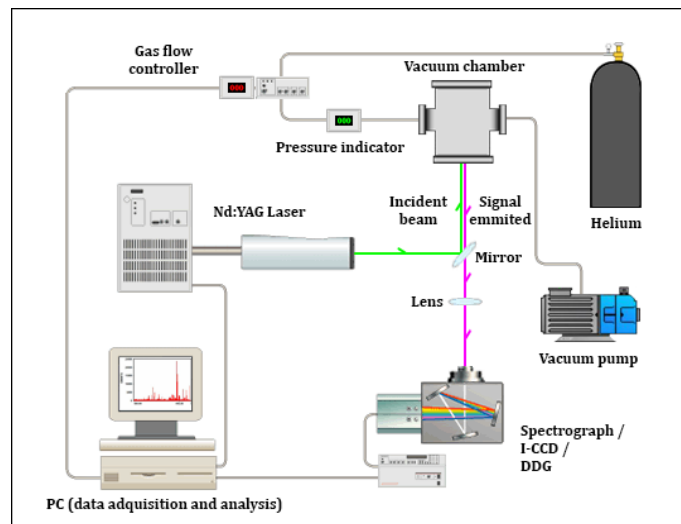
137 technique is suitable for analysis of samples [16]. They use the ratio of integral values of  
138 the chlorine spectral line to carbon spectral line for this purpose. As the concentration of  
139 chlorine could eventually change in deteriorated samples due to carbonation processes, in  
140 this work it is shown that it is advisable the normalization of the intensity of Cl atomic line  
141 by the emission of any other element present in cement (such as calcium).

142 Also, Gehlen et al. have investigated the influence of pressure and integrating time on  
143 the Cl line intensity [23]. They studied the range from 10 mbar to 320 mbar of He  
144 atmosphere, finding an optimum value at 60 mbar. In the present paper, the pressure  
145 range has been extended to 1000 bar; besides, different gas atmospheres (Air, He and Ar)  
146 have been tested in order to find the most suitable one. Labutin et al. used LIBS technique  
147 to determine chlorine in concrete in air, but they needed a double laser for this purpose  
148 [24].

149 As a main drawback of the use of LIBS technique in building materials analysis could  
150 be mentioned the low limit of detection necessary to study components at trace level, and  
151 whose corresponding emission lines are also masked in their majority by the ones of other  
152 major elements. It must be also considered the great dependence of this technique on the  
153 homogeneity of the sample, since the laser pulse impacts on the surface of the sample and  
154 create the plasma with only a few nanograms of the material, and this is going to be  
155 considered as representative of the whole. For heterogeneous samples, therefore, the  
156 technique presents major drawbacks, especially when working with a single pulse [12].  
157 This makes it necessary to perform a previous calibration of the method, as well as a  
158 treatment of the obtained data and a statistical analysis of the results, as it will be shown  
159 later in this work.

## 160 **2. Material and Method**

161 The LIBS technique has many points in common with other laser-based analytical  
162 techniques, such as Raman or fluorescence, with most of the instruments being identical.  
163 The working set-up (Fig. 2) consisted of a *Litron Nd:YAG Nano series* laser operating at  
164 532 nm wavelength, capable of generating pulses of up to 320 mJ energy with a duration  
165 of 10 ns and a frequency of 10 Hz, that were directed through a lens system towards a  
166 vacuum chamber where the sample was located. Light produced during the atomic  
167 emission was focused by another set of lenses on the detection system, consisting of an  
168 *Andor Shamrock 303* spectrograph with a grating of 1200 lines/mm and an intensified CCD  
169 (Andor iStar ICCD model DH734 18mm), operating in conjunction with a digital delay  
170 generator (DDG).



171  
172

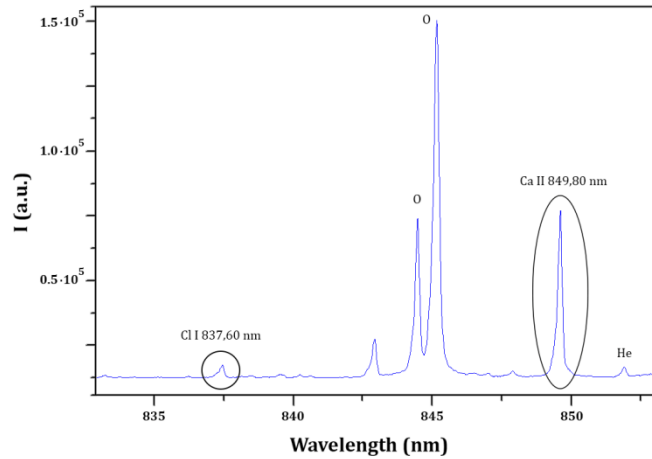
**Fig. 2** -Experimental set-up of LIBS technique.

173 LIBS measurements were performed with a delay time of 700 ns (to avoid  
174 interference of laser light), a gate time of 10  $\mu$ s and a number of accumulations of 20 per  
175 measurement.

176 For the analysis of Cl presence in mortars a vacuum system was incorporated to  
177 operate at low pressures, adding a pressure indicator inside the vacuum chamber and a  
178 digital controller for the gas flow. To carry out the optimization of system, a study of the  
179 detectable spectral lines of chlorine present in the halite (NaCl) and sylvite (KCl) minerals



180 **(Table1)** was made, taking as reference the atomic chlorine line located at 837.60 nm  
 181 **(Fig. 3)**, which had been previously established as optimal for detection in the cement  
 182 matrix [13-15].



183  
 184 **Fig. 3** – Cl I line 837,60 nm and Ca II line 849,80 nm used in LIBS measurements.

185 **Table 1** – Detectable chlorine lines in NaCl and KCl minerals.

<i>Line (nm)</i>	<i>NaCl</i>	<i>KCl</i>	<i>Ion</i>	<i>Relative intensity</i>	<i>Lower level configuration</i>	<i>Upper level configuration</i>
391,387	✓	-	Cl II	1.500	$3s^23p^3(2D^o)4p$	$3s^23p^3(2D^o)4d$
391,663	✓	-	Cl II	1.100	$3s^23p^3(2D^o)4p$	$3s^23p^3(2D^o)4d$
422,734	-	✓	Cl II	-	$3s^23p^3(2P^o)4p$	$3s^23p^3(2P^o)5s$
486,186	✓	-	Cl II	-	$3s^23p^3(2D^o)4p$	$3s^23p^3(2D^o)5s$
725,662	✓	✓	Cl I	7.500	$3s^23p^4(3P)4s$	$3s^23p^4(3P)4p$
741,411	✓	✓	Cl I	5.000	$3s^23p^4(3P)4s$	$3s^23p^4(3P)4p$
754,707	✓	✓	Cl I	11.000	$3s^23p^4(3P)4s$	$3s^23p^4(3P)4p$
771,758	✓	-	Cl I	7.000	$3s^23p^4(3P)4s$	$3s^23p^4(3P)4p$
774,497	✓	✓	Cl I	10.000	$3s^23p^4(3P)4p$	$3s^23p^4(3P)4p$
777,109	✓	✓	Cl I	650	$3s^23p^4(3P)4p$	$3s^23p^4(3P_2)4d$
808,667	✓	✓	Cl I	3.000	$3s^23p^4(1D)4s$	$3s^23p^4(1D)4p$
822,045	✓	✓	Cl I	3.000	-	-
833,331	✓	✓	Cl I	18.000	$3s^23p^4(3P)4s$	$3s^23p^4(3P)4p$
837,594	✓	✓	Cl I	99.900	$3s^23p^4(3P)4s$	$3s^23p^4(3P)4p$
842,825	✓	✓	Cl I	15.000	$3s^23p^4(3P)4s$	$3s^23p^4(3P)4p$
858,597	✓	✓	Cl I	75.000	$3s^23p^4(3P)4s$	$3s^23p^4(3P)4p$

186

187 Preparation of samples

188 For the determination of chloride ion in mortars, a set of prismatic specimens of  
 189 dimensions 40x40x160 mm were prepared following the EN 196-1:2005[16] standard.  
 190 The composition of the mass was one part of Portland CEM I42.5R/SR cement (**Table2**),  
 191 three parts of standardized CEN sand, and half part of water, resulting in a water/cement  
 192 ratio of 1/2.

193 **Table 2 – Composition of Portland CEM I42.5R/SR cement**

	<b>Cement characteristics</b>	<b>Standard</b>	<b>Usual</b>
<b>Components</b>	Clinker (%)	95-100	95
	Limestone (L) (%)	-	5
	Pozzolana (P) (%)	-	-
	Volatile ashes (V) (%)	-	-
	Steel slag (S) (%)	-	-
	Setting regulator, "plaster" (%)	-	6
<b>Chemical</b>	Sulfur trioxide (SO <sub>3</sub> ) (%)	4 max.	3,4
	Chlorides (Cl) (%)	0,10 max.	0,01
	Loss by calcination (%)	5 max.	3,1
	Insoluble residue (%)	5 max.	0,8
<b>Physical</b>	Blaine specific surface area (cm <sup>2</sup> /g)	-	3.800
	Le Chatelier expansion (mm)	10 max.	1
	Setting start time (minutes)	60 min.	130
	End time of setting	-	170
<b>Mechanical</b>	1 day compression (MPa)	-	18
	2 days compression (MPa)	20 min.	31
	7 days compression (MPa)	-	41
	28 days compression (MPa)	42-62	57
<b>Additional</b>	C3A	5 max.	3
	C3A + C4AF	22 max.	17
	Heat of hydration (J/g)		300

194  
 195 The chloride was added by dissolving several amounts of anhydrous sodium chloride  
 196 in the mixing water. The quantities were calculated on the total mass in each mix, trying to  
 197 approximate the final concentration of chlorides to certain percentages. Five mortar  
 198 samples were prepared following this procedure, with different Cl concentrations: **MS-1**,  
 199 **MS-2**, **MS-3**, **MS-4** and **MS-5** (see **Table 3**). Also, a sample with no added chlorides was  
 200 prepared to be used as blank, **MS-B**, and other sample with chloride saturated mortar for  
 201 calibration measurements, **MS-S**.

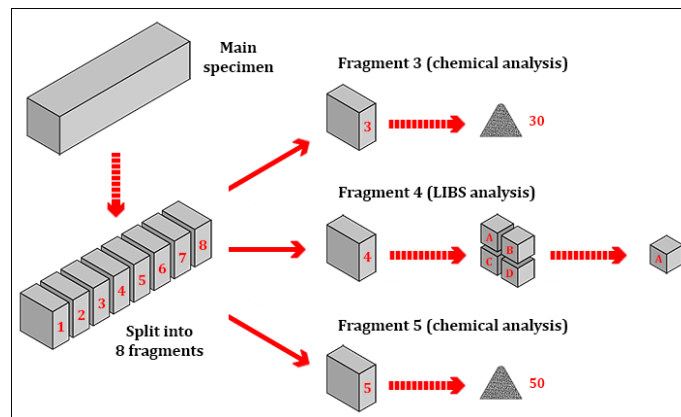
202

**Table 3** – NaCl contents and Cl percentages in cement and mortar samples.

Sample	MS-1	MS-2	MS-3	MS-4	MS-5
Total weight (gr) of NaCl anhydride	83,40	66,72	50,04	33,36	16,68
Cl content (% weight) with respect to the cement	11,37	9,10	6,82	4,55	2,27
Cl content (% weight) with respect to the mortar	2,53	2,02	1,52	1,01	0,51

203

204 Each specimen was cut transversely into eight equal portions (**Fig. 4**). Of all of them,  
 205 portions #3 and #5 were ground down for chemical analysis, which will determine the  
 206 actual concentration of chloride ion. On the other hand, portion #4 was subdivided into  
 207 four fragments, and one of them was selected to carry out LIBS analysis.



208

209

**Fig. 4** – Preparation of mortar samples.

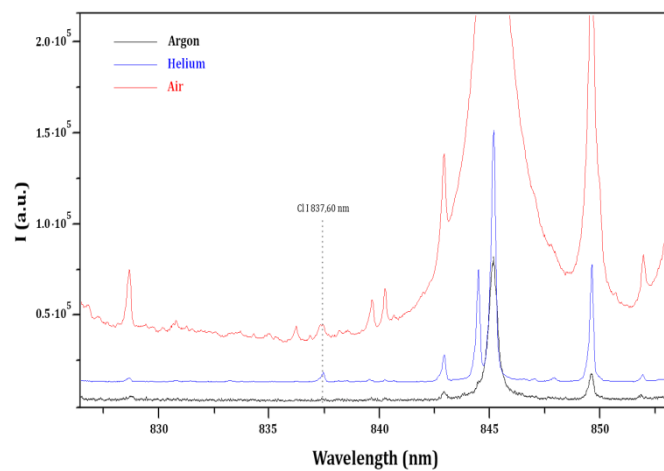
### 210 2.1 Optimization of measurement parameters

211 Previous to LIBS analysis of the mortar specimens, a series of tests were carried out to  
 212 optimize the variables that affect the measurements, in order to perform the analysis  
 213 under the best possible conditions. These tests address the parameters corresponding to  
 214 the gas pressure at which the measurements were made, and the composition of the gas  
 215 used for the plasma creation.

216 To carry out these calibration tests, the sample of chloride-saturated mortar **MS-S**  
217 was used, as it provides intense and well-defined spectral lines in which it is easier to  
218 observe variations in intensity.

### 219 2.1.1 Gas atmosphere composition

220 Measurements were made in air, argon and helium atmospheres, respectively, in  
221 order to find the best condition for chlorine detection (**Fig. 5**).



222  
223 **Fig. 5** –Comparison of LIBS measurements in Argon, Helium and Air atmospheres.

224 Air provides the highest LIBS signal, but it is composed by a set of atoms and  
225 molecules (such as O<sub>2</sub>) whose emission signals interfere with those of Cl line. To avoid this  
226 overlapping becomes particularly important when the element to be analyzed is at trace  
227 level, as it is the case of the chloride ion in mortars.

228 Argon and helium are simpler gases, whose emission lines barely interfere with the  
229 signal of the sample. But, as it is shown in figure 5, in argon atmosphere the emission of Cl  
230 I 837.60 nm line has a lower signal compared to that detected in a helium one. This fact is  
231 due to the higher ionization energy of helium ( $E_{i,Ar} = 15.75$  eV,  $E_{i,He} = 24.59$  eV), and so the  
232 greater excitation capacity of the helium plasma. For this reason, a helium atmosphere  
233 was chosen in the LIBS set-up proposed in this work.

### 234 2.1.2 Pressure optimization

235 Atmospheric gas pressure is a factor that directly affects the quality of the  
236 measurement. High pressure leads to a greater gas abundance in the environment and  
237 therefore to more intense emissions corresponding to this gas. This can be inconvenient  
238 when trying to analyze trace elements, with a dimmed emission that could be masked. On  
239 the other hand, at low pressure the population of emitting species is low, and so is the  
240 signal detected.

241 To figure out the optimum pressure value for the Cl determination in mortars, a set of  
242 measurements varying this parameter were made for the sample **MS-S**, using a helium  
243 atmosphere. The line used as reference was Cl I 837.60 nm, corresponding to radiative  
244 transitions between atomic chlorine levels.

245 Measurements were performed increasing the pressure gradually by steps of 50 mbar  
246 covering the range of values between 50 and 1000 mbar.

247 **Fig. 6** represents the normalized intensity versus pressure, where normalization was  
248 carried out from peak ( $I$ ) and background ( $B$ ) signals, and  $\frac{I-B}{B}$ . The fitting to a Boltzmann  
249 sigmoidal function is also shown in this figure. There, it is shown how the line intensity  
250 undergoes an increase with the pressure until stabilizing from 400 mbar. This stabilization  
251 corresponds to the dependence of discharge parameters (such as the electron density) on  
252 the pressure-[14]. It is well-known that electrons have a high influence on the excitation  
253 capacity of the discharge.

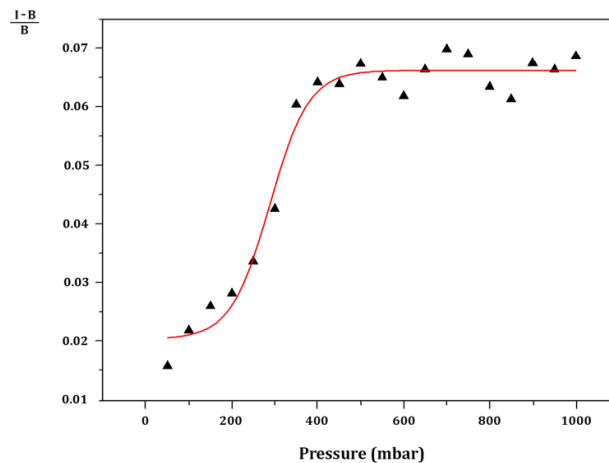


**Fig. 6** – Dependence of normalize intensity of Cl I line 837,60 nm on He atmosphere pressure.

254  
255  
256

257 Thus, for the determination of chloride in mortars by the proposed LIBS technique, a  
258 working pressure of 1000 mbar will be established as the optimum measurement value, as  
259 it is easier to keep the pressure stabilized at this value rather than at lower ones.

## 260 2.2 Chemical analysis and EDX

261 While portion #4 of each mortar specimen was used in LIBS analysis, the immediately  
262 preceding and subsequent portions #3 and #5 were ground to particles less than 250  $\mu\text{m}$   
263 size. From them, samples labeled as #30 and #50 were taken to perform chemical analysis  
264 in order to determine the exact concentration of chloride ion.

265 The Volhard's method was used for this purpose, following the procedure described  
266 in EN 196-2:2013 [17] standard. However, since this standard is designed for samples with  
267 a much lower chloride concentration, when applied to the mortar samples in this work  
268 results were out of range. For this reason, the quantities of reagents indicated in the  
269 standard were modified and adapted to the high concentrations of chloride ion in the  
270 samples. Thus, to an amount of  $0.5 \pm 0.05$  g of sample, 50 ml of distilled water and 50 ml of  
271  $\text{HNO}_3$  diluted to 1:2 were added, boiling for 2 minutes. After this, 20 ml of 0.1M  $\text{AgNO}_3$   
272 solution was added, boiling again for another 2 minutes. The solution was then filtered,

273 washing with HNO<sub>3</sub> diluted to 1:100 until the filtrated volume and wash water were  
274 around 200 ml. The solution was subsequently cooled below 25°C in the absence of light,  
275 and 5 ml of NH<sub>4</sub>Fe(SO<sub>4</sub>)<sub>2</sub> indicator solution were added, carrying out the titration with a  
276 0.05M NH<sub>4</sub>SCN solution.

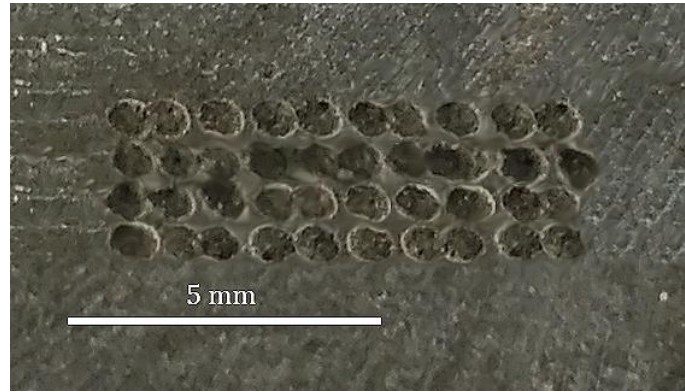
277 The chloride content of each sample was calculated according to the following  
278 equation:

$$279 \quad [Cl^-] = 7.092 \times \frac{(V_B - V_S)}{V_B \times m_S} \quad (5)$$

280 Where  $m_S$  is mass (in grams) of sample used in the analysis;  $V_S$  and  $V_B$  are volumes of  
281 thiocyanate solution consumed by the sample and by the blank, respectively, in  
282 millimeters.

283 Chemical analysis was carried out in triplicate for all mortar samples, as well as the  
284 analysis of one blank for each sample. Finally, averaged values of the chlorine ion  
285 concentration for the pairs of samples #30 and #50 belonging to the same specimen were  
286 obtained.

287 As an instrumental contrast analysis, an EDX analysis was performed in the same area  
288 of the samples where the LIBS analysis was performed (**Fig.7-8**). The electron microprobe  
289 technique was implemented on a JEOL JSM-7800F scanning electron microscope using an  
290 acceleration voltage of 15 kV and a working distance of 10 mm. The X-ray detector was an  
291 X-MaxN150 from Oxford Instruments.

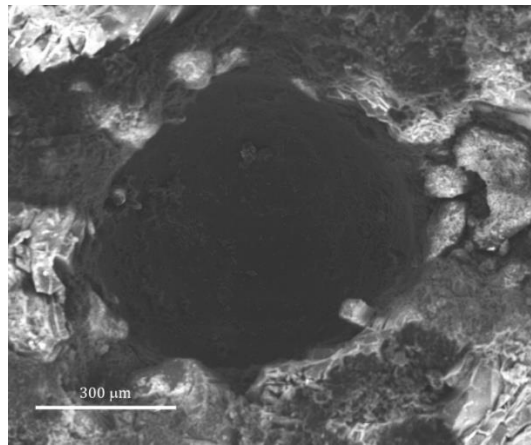


292

293

294

**Fig. 7** – Image of laser impact distribution on sample surface obtained with the electron microscope used in EDX analysis.



295

296

297

**Fig. 8** – In-detail image of laser impact on sample surface obtained with the electron microscope used in EDX analysis.

298

### 3. Results

299

#### 3.1 Chemical analysis and EDX

300

301

302

303

304

The average concentration of chloride obtained by the chemical analysis in all the samples is shown in **Table 4**. Comparison between the theoretical concentration predicted in the preparation of the test specimens and the actual concentration obtained in the chemical analysis can be found in **Fig. 9**. A gradual decrease of half point of percentage in the concentration of chloride ion between samples is observed.

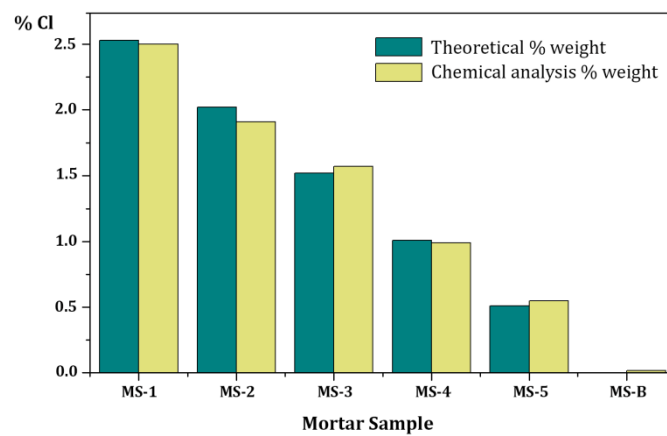
305

**Table 4** – Results of Cl concentration obtained from chemical analysis.



306  
307  
308  
309  
310  
311  
312  
313

Sample	Cl content (% weight) with respect to the mortar
MS-1	2,50% ± 0,17%
MS-2	1,91% ± 0,06%
MS-3	1,57% ± 0,12%
MS-4	0,99% ± 0,05%
MS-5	0,55% ± 0,07%
BLANK	0,02% ± 0,00%



314  
315  
316

**Fig. 9** – Comparison between theoretical Cl concentration and chemical analysis in the different samples.

317  
318  
319  
320

On the other hand, the results obtained of EDX measurements are shown in **Table 5**. A good agreement between the Cl concentration values obtained by EDX for each sample and those provided by the chemical analysis is obtained, confirming the accuracy of results obtained through the chemical analysis.

321

**Table 5** – Results of Cl concentration obtained from EDX analysis

Sample	Cl content (% weight) with respect to the mortar
MS-1	2,56% ± 0,04%
MS-2	1,95% ± 0,03%
MS-3	1,49% ± 0,03%

322	<b>MS-4</b>	1,02% ± 0,03%
323	<b>MS-5</b>	0,44% ± 0,02%

---

324  
325  
326  
327  
328

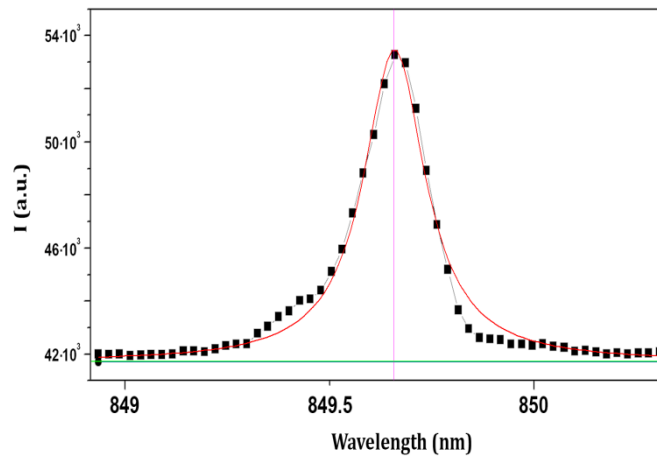
### 329 3.2 LIBS analysis of the mortar samples

330 LIBS study of the mortar samples was performed on one of the inner faces of fragment  
331 A of portion #4 of each one of the specimens corresponding to the different concentrations  
332 prepared for the tests. For each sample, 40 determinations were made at different points,  
333 with 20 accumulations for each determination. **Fig. 7** shows image of the different spots of  
334 typical LIBS measurement. The area of the region affected when taking forty  
335 measurements was under 1 cm<sup>2</sup>. In-detail spot obtained with electron microscope used in  
336 EDX analysis is shown in **Fig. 8**. Spots under 1 mm of diameter and deep were observed,  
337 which means damages in the mortar lower than 3 mg by shot and, for typical  
338 measurement of 40 determinations, a total damage lower than 0.12 g. Thus, the degree of  
339 damage is significantly lower than that produced by other techniques. The minimum  
340 amount of mortar required for chemical analysis was 5 g per point according to EN 196-  
341 2:2013 [26]. In this sense, LIBS has been considered as a non-destructive technique and  
342 used in analysis of valuables, such as archeological remains and art treasures.

343 The determinations with a low or zero intensity in Ca ion lines have been  
344 discriminated, since they represent zones of the sample where the siliceous phase (free  
345 from the presence of chlorides) of the sample predominates.

346 Measured spectral zone included the reference line Cl I 837.60 nm, and a line  
347 representative of present cement, the Ca II849.80 nm line (**Fig. 3**). In each determination,

348 the ratio of the areas of both chlorine and the calcium ion lines (*Cl/Ca ratio*) was obtained  
349 by calculating of their peak area fitting to a Voigt function (**Fig. 10**). Absolute intensities  
350 of these lines depend on detection conditions and can vary for every measurement, but  
351 their ratio *Cl/Ca*, only depends on the chloride ion concentration of the sample. This is  
352 based on the fact that the area of the chlorine line accounts for the concentration of  
353 chloride in the sample, whereas the area of the calcium ion peak is a function of the  
354 amount of cement used in the preparation of the test pieces, the same in all of them, and  
355 therefore constant.



356  
357

**Fig. 10** – Voigt profile fitting to Ca II line 849,80 nm for area calculation.

358 Consistent with the fact that samples are not homogeneous, Cl concentrations and  
359 results vary from point to point. LIBS measurements give information of a reduced extent  
360 of about 300  $\mu\text{m}$  (see **Fig. 8**). In order to obtain representative results for total sample, a  
361 statistical study of several data (40 measurements by sample), was done (see **Fig. 7**).

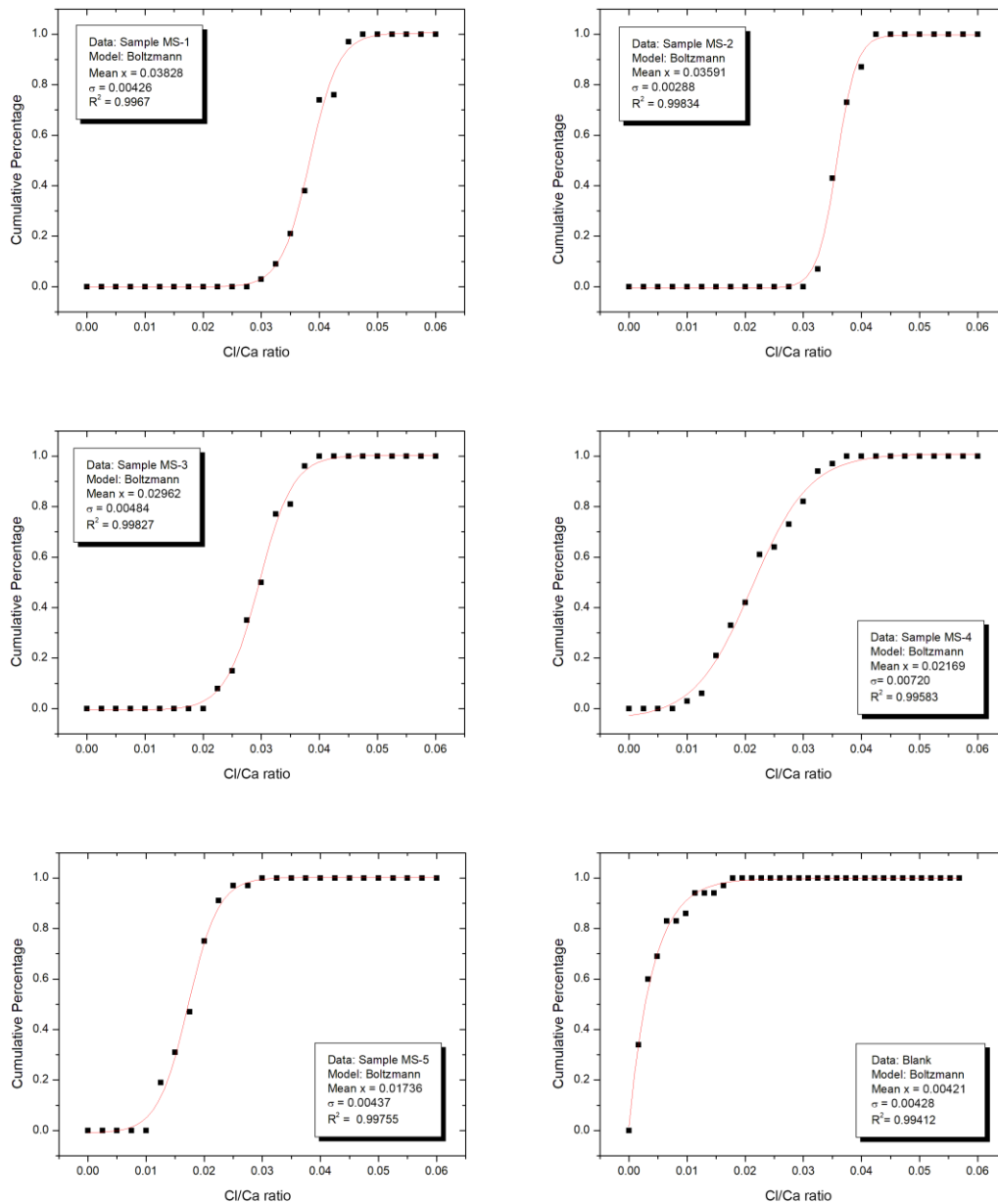
362 This number of data is too low to be enough to directly prove that its frequency  
363 follows a normal distribution. For this reason, the cumulative percentage was used in the  
364 statistical study. **Fig. 11** shows cumulative percentage of data obtained from MS-1 to MS-  
365 5 samples. This percentage fits well with the Gauss error function corresponding to the  
366 normal distribution:

367 
$$errf(x) = \frac{1}{\sigma\sqrt{2}} \int_{-\infty}^x e^{-(x'-\mu)^2/2\sigma^2} dx' \quad (6)$$

368 All R<sup>2</sup> coefficients of these fittings are higher than 0.994, showing that data  
 369 distributions correspond to a normal type distribution with mean values and standard  
 370 deviations included in figure 11. **Table 6** gathers mean values and error of Cl/Ca ratio  
 371 from LIBS analysis.

372 **Table 6** – Results of mean Cl/Ca ratio and error obtained from LIBS analysis

373	<b>Sample</b>	<b>Cl/Ca peak area ratio</b>
374	<b>MS-1</b>	0,038288 ± 0,004262
375	<b>MS-2</b>	0,035909 ± 0,002883
376	<b>MS-3</b>	0,029625 ± 0,004837
377	<b>MS-4</b>	0,021689 ± 0,007199
378	<b>MS-5</b>	0,017360 ± 0,004374
379	<b>BLANK</b>	0,004214 ± 0,004289



380

381

**Fig. 11** – Cumulative percentage of LIBS measurement data for the different samples together its fitting to a Gauss error function.

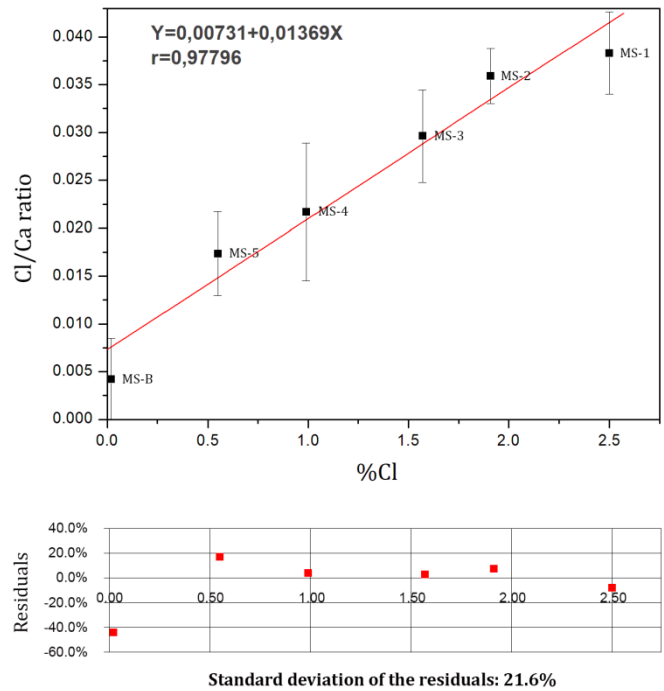
382

383

Figure 12 depicts the mean Cl/Ca ratio obtained from the LIBS versus the actual chloride concentration provided by the chemical analysis. A linear relationship was found, which shows that despite the variation in the peak intensity for different measurements of the same sample, the mean Cl/Ca ratio retains a direct proportionality with respect to the chloride content of the sample.

387

388 **Fig. 12** shows the calibration curve obtained from linear fitting of experimental data  
 389 together with its residuals. This is an essential stage for determination of Cl concentration  
 390 by LIBS technique. A regression factor of 0.977 and a standard deviation of the residuals of  
 391 21.6% are obtained, which ensures the goodness of the calibration process. This curve will  
 392 be used in next section for the determination of Cl concentrations in unknown samples.



393  
 394 **Fig. 12** – Calibration curve and residual plots for LIBS technique obtained from the  
 395 linear least squares regression of mean Cl/Ca ratio vs Cl concentration.

396 **3.3 Analysis of specimens submerged in saturated sea salt water**

397 In order to compare the applicability of LIBS analysis in the study of chloride ion  
 398 penetration in real mortar samples, a sample subjected to the continuous action of the  
 399 chloride ion was analyzed. For this purpose, a chloride-blank mortar specimen was used.  
 400 This specimen had been submerged in water saturated with sea salt for a period of sixty  
 401 months.

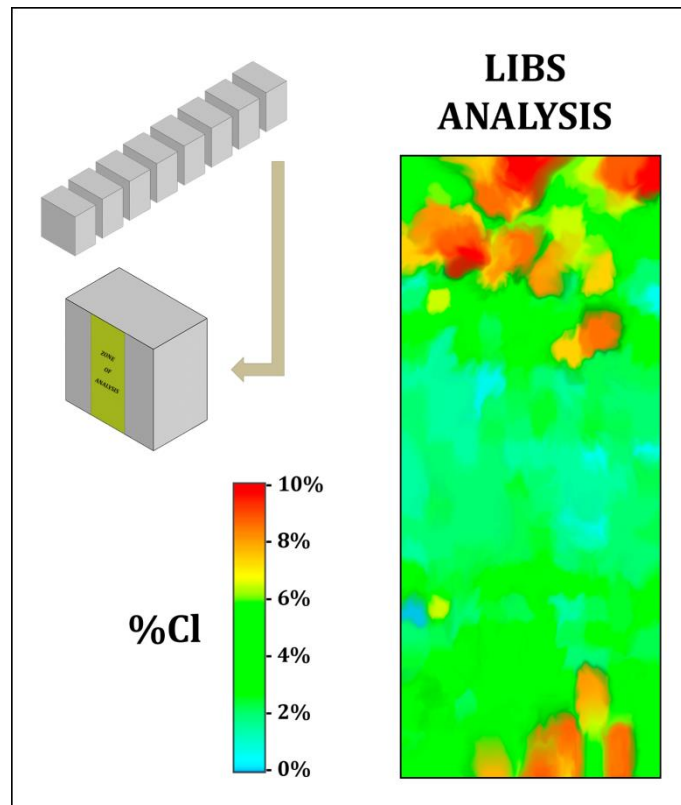
402 After that period, the specimen was divided into eight fragments following the  
 403 procedure previously described, and three of the inner fragments were analyzed by LIBS  
 404 (**MSW-1, MSW-2 and MSW-3**). The averaged values of chlorine concentration for each of  
 405 the fragments are gathered in **Table 7** which also includes the values obtained through  
 406 chemical analysis. It can be observed that, due to the heterogeneity of the samples, the  
 407 results obtained by LIBS present a higher standard deviation. However, results from LIBS  
 408 analysis present a great similarity with those measured by chemical analysis.

409 **Table 7** – Comparison of LIBS results and chemical analysis in submerged samples

410	<b>Sample</b>	<b>Average %Cl LIBS</b>	<b>Average %Cl Chemical</b>
411	<b>MSW-1</b>	1,90 ± 0,27	1,91 ± 0,08
412	<b>MSW-2</b>	2,43 ± 0,32	2,05 ± 0,08
413	<b>MSW-3</b>	2,33 ± 0,31	2,03 ± 0,08

414 In order to study the penetration of chlorine into the cement matrix, another  
 415 fragment of the mortar sample submerged in saturated chloride solution was analyzed by  
 416 LIBS. This time the analysis was restricted to the innermost part of the fragment, the  
 417 analysis zone being limited to a strip of 10 mm width by the 40 mm height of the fragment  
 418 (**Fig. 13**).

419 **Fig. 13** shows the distribution of the chlorine concentration in the sample measured  
 420 from LIBS analysis. It can be seen “channels” through which chlorine penetrates in the  
 421 mortar sample. Cl concentrations are highest at top and bottom zones, due to both faces  
 422 were in direct contact with the saturated solution, especially the top zone since the bottom  
 423 one was resting on the treatment container.



424

425 **Fig. 13** – Chlorine distribution inside a mortar sample submerged in water saturated

426 with sea salt for 60 months obtained from LIBS analysis.

427 Thus, this study shows LIBS analysis provides much detailed information about the

428 sample due to its high resolution, being able to perform a mapping of the concentration of

429 chloride ion on the analyzed surface. It has the added advantages of being a non-

430 destructive technique and allowing to work on-site. Definitely, this technique can help to

431 diagnose the deterioration state of construction materials through the determination of Cl

432 concentration in these materials.

#### 433 **4. Conclusions**

434 This work aims to contribute to the development of an optimum LIBS technique,

435 allowing for detection and measurement of chlorine in mortars and so, estimate of the

436 deterioration state of this material.



437 The set-up and the optimum conditions for LIBS analysis of mortar samples have been  
438 described. Unlike previous studies of other authors, pressures above 400 mbar have been  
439 found as optimum for obtaining highest intensities of Cl atomic lines. Different gas  
440 atmospheres have been tested, and the use of helium gas has been shown to be best to give  
441 clearest spectra without line overlapping.

442 In this work, the ratio between area of chlorine atomic line 837.60 and line, calcium  
443 (one of the cement components) ion line 849.80 nm, is used. This parameter gives more  
444 accurate results, as concentration of calcium is considered constant in every kind of  
445 mortar. Different measurements in a small area of about 25 mm<sup>2</sup> of mortar have shown  
446 that ratio values follow a normal distribution whose mean and standard deviation give the  
447 representative value of the measure and its error. A linear correlation has been found  
448 between the average results obtained from LIBS and the concentration of chloride,  
449 obtained by chemical analysis, which allows to get a calibration curve for analytical use of  
450 this technique. This calibration curve depends on mortar composition, in particular, the Ca  
451 concentration in the material, which depends on type of cement used. The curve obtained  
452 in this work is valid for a mortar prepared with Portland CEM I42.5R/SR cement following  
453 procedure in EN 196-1:2005 standard. For a practical implementation of this technique to  
454 actual cases, different calibration curves would be needed for each kind of standard  
455 mortar.

456 To the best of the authors' knowledge, this work reports for the first time on the  
457 comparison of LIBS technique results and those obtained with other spatially resolved  
458 technique, EDX. A very good agreement has been found between results from LIBS, EDX  
459 and chemical analysis.

460 It has also been demonstrated that the LIBS technique developed in this paper is  
461 suitable for the qualitative and quantitative analysis of chlorine concentration in  
462 deteriorated building materials such as mortars and concretes. LIBS technique has been

463 validated from the study of chloride penetration in a sample of mortar subjected to the  
464 action of water saturated with sea salt.

465 Compared to classical chemical methods, the LIBS technique provides more  
466 information and has the advantage of being a non-destructive technique with the ability to  
467 perform on-site analysis.

468 In further work, the possibility of developing a mobile device based on LIBS technique  
469 will be studied. This device will allow *in-situ* evaluation of building and construction  
470 structures. The possibility to integrate laser, spectrometer and CCD in a single device will  
471 allow to reduce set-up costs. A first estimation of its cost is about 50.000 \$. On the other  
472 hand, having a collection of calibration curves for the different types of standard mortar,  
473 all process (measurements, peak integration and determination of Cl concentration) could  
474 be automated, and no highly specialized personnel will be necessary for its use.

## 475 **5. Acknowledgements**

476 Authors thank the European Regional Development Funds program (EU-FEDER) and  
477 the MINECO (project MAT2016-79866-R) for financial support. The authors also are  
478 grateful to Andalusian Regional Government (Research Group FQM-136) and to the  
479 Research Plan of the University of Cordoba (2017) for their technical and financial  
480 support. The authors wish to thank the staff at the Electron Microscopy and Elemental  
481 Analysis units of the Central Research Support Service (SCAI) of the University of Cordoba  
482 for technical assistance.

## 483 **REFERENCES**

484 **[1]** A. Neville, *Chloride attack of reinforced concrete: an overview*, Mater. Struct. 28  
485 (1995) 63-70.

- 486 [2] M.F. Montemor, A.M.P. Simões, M.G.S. Ferreira, *Chloride-induced corrosion on*  
487 *reinforcing steel: from the fundamentals to the monitoring techniques*, *Cement*  
488 *Concrete Comp.* 25 (2003) 491-502.
- 489 [3] G.K. Glass, N.R. Buenfeld, *The presentation of the chloride threshold level for corrosion*  
490 *of steel in concrete*, *Corros. Sci.* 39 (1997) 1001-1013.
- 491 [4] M.C. Alonso, M. Sánchez, *Analysis of the variability of chloride threshold values in the*  
492 *literature*, *Mater. Corros.* 60 (2009) 631-637.
- 493 [5] L. Radziemski, D. Cremers, *A brief history of laser-induced breakdown spectroscopy:*  
494 *From the concept of atoms to LIBS 2012*, *Spectrochim. Acta B* 87 (2013) 3-10.
- 495 [6] DW. Hahn, N. Omenetto, *Laser-Induced Breakdown Spectroscopy (LIBS), Part II:*  
496 *Review of Instrumental and Methodological Approaches to Material Analysis and*  
497 *Applications to Different Fields*, *Appl. Spectrosc.* 66 (2012) 347,419.
- 498 [7] R. Noll, C. Fricke-Begemann, M. Brunk, S. Connemann, C. Meinhardt, M. Scharun, V.  
499 Sturm, J. Makowe, C. Gehlen, *Laser-induced breakdown spectroscopy expands into*  
500 *industrial applications*, *Spectrochim. Acta B* 93 (2014) 41-51.
- 501 [8] P. Pořízka, A. Demidov, J. Kaiser, J. Keivanian, I. Gornushkin, U. Panne, J. Riedel,  
502 *Laser-induced breakdown spectroscopy for in situ qualitative and quantitative*  
503 *analysis of mineral ores*, *Spectrochim. Acta B* 101 (2014) 155-163.
- 504 [9] S. Guirado, F.J. Fortes, V. Lazic, J.J. Laserna, *Chemical analysis of archeological*  
505 *materials in submarine environments using laser-induced breakdown spectroscopy.*  
506 *On-site trials in the Mediterranean Sea*, *Spectrochim. Acta B* 74-75 (2012) 137-143.
- 507 [10] J.L. Gottfried, F.C. De Lucia Jr, C.A. Munson, A.W. Miziolek, *Laser-induced breakdown*  
508 *spectroscopy for detection of explosives residues: a review of recent advances,*  
509 *challenges, and future prospects*, *Anal. Bioanal. Chem.* 395 (2009) 283-300.
- 510 [11] E.M. Rodriguez-Celis, I.B. Gornushkin, U.M. Heitmann, J.R. Almirall, B.W. Smith, J.D.  
511 Winefordner, N. Omenetto, *Laser induced breakdown spectroscopy as a tool for*

512 *discrimination of glass for forensic applications*, Anal. Bioanal. Chem. 391 (2008)  
513 1961-1968.

514 [12]Anna P.M. Michel, *Review: Applications of single-shot laser-induced breakdown*  
515 *spectroscopy*, Spectrochim. Acta B 65 (2010) 185-191.

516 [13]A. Uhl, K. Loebe, L. Kreuchwig, *Fast analysis of wood preservers using laser induced*  
517 *breakdown spectroscopy*, Spectrochim. Acta B 56 (2001) 795-806.

518 [14]P. Inakollu, T. Philip, AK. Rai, FY, Yueh, JP. Singh, *A comparative study of laser induced*  
519 *breakdown spectroscopy analysis for element concentrations in aluminum alloy*  
520 *using artificial neural networks and calibration methods*, Spectrochim. Acta B 64  
521 (2009) 99-104.

522 [15]J. El Haddad, M. Villot-Kadri, A. Ismael, G. Gallou, K. Michel, D. Bruyere, V. Laperche,  
523 L. Canioni, B. Bousquet, *Artificial neural network for on-site quantitative analysis of*  
524 *soils using laser induced breakdown spectroscopy*, Spectrochim. Acta B 79-80  
525 (2013) 51-57.

526 [16]G. Wilsch, F. Weritz, D. Schaurich, H. Wiggenhauser, *Determination of chloride*  
527 *content in structures with laser-induced breakdown spectroscopy*, Constr. Build.  
528 Mater. 19 (2005) 724-730.

529 [17]F. Weritz, S. Ryahi, D. Schaurich, A. Taffe, G. Wilsch, *Quantitative determination of*  
530 *sulfur content in concrete with laser-induced breakdown spectroscopy*, Spectrochim.  
531 Acta B 60 (2005) 1121,1131.

532 [18]F. Weritz, A. Taffe, S. Dieter, G. Wilsch, *Detailed depth profiles of sulfate ingress into*  
533 *concrete measured with laser induced breakdown spectroscopy*, Constr. Build. Mater.  
534 23 (2009) 275-283.

535 [19]A. Mansoori, B. Roshanzadeh, M. Khalaji, SH. Tavassoli, *Quantitative analysis of*  
536 *cement powder by laser induced breakdown spectroscopy*, Opt. Laser. Eng. 49 (2011)  
537 318-323.

- 538 [20]I. Gaona, P. Lucena, J. Moros, *Evaluating the use of standoff LIBS in architectural*  
539 *heritage: surveying the Cathedral of Malaga*, J. Anal. At. Spectrom. 28 (2013) 810-  
540 820.
- 541 [21]M. Brai, G. Gennaro, T. Schillaci, *Double pulse laser induced breakdown spectroscopy*  
542 *applied to natural and artificial materials from cultural heritages. A comparison*  
543 *with micro-X-ray fluorescence analysis*, Spectrochim. Acta B 64 (2009) 1119-1127.
- 544 [22]MA. Gondal, ZH. Yamani, T. Hussain, OSB, Al-Amoudi, *Determination of Chloride*  
545 *Content in Different Types of Cement Using Laser-Induced Breakdown Spectroscopy*,  
546 Spectrosc. Lett. 42 (2009) 171-177.
- 547 [23]C. Gehlen, E. Wiens, R. Noll, G. Wilsch, K. Reichling, *Chlorine detection in cement with*  
548 *laser-induced breakdown spectroscopy in the infrared and ultraviolet spectral range*,  
549 Spectrochim. Acta B 64 (2009) 1135-1140.
- 550 [24]T.A. Labutin, A.M. Popov, S.N. Raikov, S.M. Zaytsev, N.A. Labutina, N.B. Zorov,  
551 *Determination of chlorine in concrete by laser-induced breakdown spectroscopy in*  
552 *air*, J. Appl. Spectrosc. 80 (2013) 315-318.
- 553 [25]European Standard EN 196-1:2005, *Methods of testing cement. Determination of*  
554 *strength* (2005).
- 555 [26]European Standard EN 196-2:2013, *Method of testing cement. Chemical analysis of*  
556 *cement* (2013).